Seminar Report on Grid Cells Project

Tymur Mykhailevskyi
7031100
University of Saarland
tymy00001@stud.uni-saarland.de

Abstract

This is a seminar report on the project dedicated to deepen the understanding of grid cells. The main focus of the report was to slightly modify the methodology of the original paper by Chaplot, Parisotto, and Salakhutdinov (2018), which presents RNN path integration along with interpretability of the model. The initial idea was to train a more robust model that would be able to generalize better, therefore, mimicking closer to how the real grid cells would appear. However, the results were not as expected and even the initial replication of the original paper was not entirely successful. The report shows in detail the steps taken to achieve the results, as well as the problems faced during the project. In addition, some future directions are discussed. All code is available via Mykhalievskyi (2025).

1 Introduction

The brain's ability to navigate and understand spatial environments is a complex and fascinating process that has been the subject of extensive research in neuroscience. The main parts of the brain responsible for spatial navigation are the hippocampus and the entorhinal cortex. Within these regions a number of specialized neurons have been identified, including speed cells, head direction cells, border cells, grid cells and place cells.

Grid cells play a crucial role in navigation and spatial memory by providing a coordinate system for the brain to represent space. Understanding how grid cells work and how they are organized is a key challenge in neuroscience. The main focus of this report is on grid cells, which are a type of neuron that fire in a hexagonal pattern as an animal moves through space. They were first discovered in the entorhinal cortex of rats by Hafting, Fyhn, Molden, Moser, and Moser (2005) and have since been found in other species, including humans. Grid cells are thought to provide a metric for spatial navigation, allowing animals to estimate their position and distance from landmarks in their environment.

The original paper by Chaplot et al. (2018) presents a model of brain cells responsible for spatial navigation using recurrent neural networks (RNNs) and explores the interpretability of the model. The goal of this seminar report is to build upon this work by modifying the methodology to improve the model's performance and interpretability. The absence of the original codebase made the replication of the results more challenging.

2 Methodology

The methodology of the original paper by Chaplot et al. (2018) involves training a recurrent neural network (RNN) to perform path integration, which is the process of estimating one's position based on self-motion cues. The RNN is trained using a dataset of simulated trajectories, where the input to the network is a sequence of speed and direction signals, and the output is the estimated position of the agent by x and y coordinates. The RNN architecture consists of a single hidden layer with 100

Preprint. Under review.

units and uses a tanh activation function. The network is trained using backpropagation through time (BPTT) with a mean squared error loss function extended with a regularization term to encourage sparsity in the hidden layer activations.

2.1 Dataset

The dataset used in the original paper was generated by "modified Brownian motion to increase the probability of straight-runs" (Chaplot et al., 2018). Due to the ambiguity of this description and the absence of the original codebase, a different approach was taken.

2.1.1 Agent motion model

The agent motion model is based on a combination of Ornstein-Uhlenbeck process for speed dynamics and von Mises distribution for heading dynamics. The speed dynamics are modeled as a stochastic process that tends to revert to a mean speed over time. The heading dynamics are modeled using the von Mises distribution, which is a circular distribution that is often used to model angles. The position of the agent is updated based on its speed and heading at each time step. The mathematical formulation of the agent motion model is as follows:

$$\text{Speed dynamics:} \quad x_{t+1} = \begin{cases} x_t + \theta_s(\mu_s - x_t)\,\Delta t + \sigma_s\sqrt{\Delta t}\,\eta_t, & \text{if } u_t < p_{\text{change}}, \\ x_t, & \text{otherwise,} \end{cases} \tag{1}$$

$$\eta_t \sim \mathcal{N}(0,1), \quad u_t \sim \mathcal{U}(0,1) \tag{2}$$

$$v_{t+1} = v_{\min} + (v_{\max} - v_{\min}) \cdot \frac{1}{1 + e^{-x_{t+1}}} \tag{3}$$

$$\text{Heading dynamics:} \quad \Delta\phi_{t+1} \sim \text{vonMises}(0, \kappa), \tag{4}$$

$$\phi_{t+1} = \phi_t + \Delta\phi_{t+1} \tag{5}$$

$$\text{Position update:} \quad \mathbf{r}_{t+1} = \mathbf{r}_t + v_{t+1}\,\Delta t \begin{pmatrix} \cos\phi_{t+1} \\ \sin\phi_{t+1} \end{pmatrix} \tag{6}$$

The Table 1 summarizes the parameters used in the agent motion model, as well as the range in which they were uniformly sampled for each agent.

Table 1: Rat movement model parameters and their sampled ranges.

Parameter	Description	Range
$v_{\min}$	Minimum possible speed (units/s)	$[0.02,\ 0.10]$
$v_{\max}$	Maximum possible speed (units/s)	$[0.60,\ 0.80]$
Δt	Simulation time step (s)	0.1
θ_s	Rate of reversion of latent speed toward μ_s	$[0.20,\ 0.40]$
μ_s	Long-term mean of latent speed variable	0
σ_s	Standard deviation of speed noise term	$[0.30,\ 0.50]$
κ	Directional persistence (von Mises concentration)	$[4,\ 10]$
p_{change}	Probability of speed update per step	$[0.10,\ 0.20]$

2.1.2 Environment and trajectories

Initially the idea was to make more complex environments specifying number of corners and two radiuses, the corners being randomly generated along the ring defined by the two radiuses. However, due to the complexity of the task and time constraints, the trained models only used square and equilateral triangle environments fit in a unit circle. The agent was initialized at (0, 0) position and direction of 0 radians. Each trajectory consisted of 20 to 50 steps. In case of agent going out of

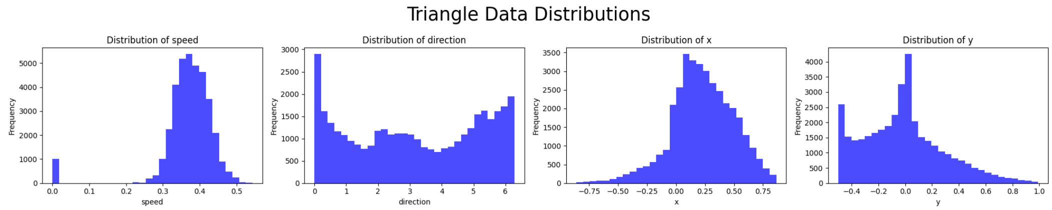

Figure 1: Triangle environment data distributions for speed, direction, x and y coordinates.

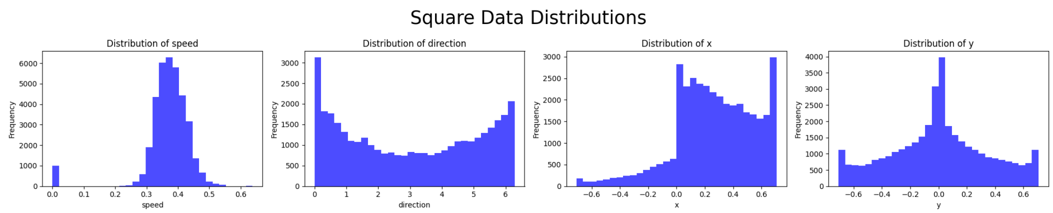

Figure 2: Square environment data distributions for speed, direction, x and y coordinates.

bounds of the environment, the current step was discarded and a new step was generated until the agent stayed within the environment limits, following the original paper's approach.

Two datasets were created - one for each type of environment. 50 different agents were simulated for each environment, with each agent having its own set of parameters sampled from the ranges specified in Table 1. For each agent, 20 trajectories were generated, resulting in a total of 1000 trajectories per environment type.

2.1.3 Data distributions

In order to further investigate the generated datasets, the distributions of speed, direction, x and y coordinates were plotted for both environments. The plots are shown in Figures 1 and 2. Note that each trajectory starts from an initial identical step of (0,0) position, 0 radians direction and 0 speed, which is reflected in the distribution.

Due to the stochastic nature of the agent motion model, the distributions of speed is similar across both environments, with most speeds being concentrated around the mean speed of approximately 0.4 units/s. The direction distributions are slightly different due to the geometry of the environments and the resampling technique used when the agent goes out of bounds. Similarly to the direction distributions, the x and y coordinate distributions are also affected by the geometry of the environments and the initialization of the agent at the center of the environment always facing the same direction.

3 RNN model training

The RNN model architecture and training procedure closely followed the original paper by Chaplot et al. (2018). The model consisted of a single hidden layer with 100 units and used a tanh activation function. The input to the network was a sequence of speed and direction signals, and the output was the estimated position of the agent in x and y coordinates. The model was trained using backpropagation through time (BPTT) with a mean squared error loss function extended with a regularization term to encourage sparsity in the hidden layer activations.

$$x_0 = 0, \quad u_0 = \tanh(x_0) = 0, \tag{7}$$

$$x_t = x_{t-1} + \frac{\Delta t}{\tau}\left(-x_{t-1} + W_{\text{rec}} u_{t-1} + W_{\text{in}} I_t + b + \xi_t\right), \quad \xi_t \sim \mathcal{N}(0, \sigma^2 I), \tag{8}$$

$$u_t = \tanh(x_t), \tag{9}$$

$$y_t = W_{\text{out}} u_t \tag{10}$$

Equation 7 shows the initialization of the RNN's hidden state, where x_0 is the initial hidden state vector, and u_0 is the initial activation vector obtained by applying the tanh activation function to x_0, ensuring that the initial prediction aligns with the starting position of the agent at the origin.

Equation 8 describes the update of the hidden state at each time step t. The hidden state x_t is updated based on the previous hidden state x_{t-1}, the recurrent weights W_{rec}, the input weights W_{in}, the input vector I_t (which includes speed and direction), a bias term b, and a noise term ξ_t sampled from a Gaussian distribution with mean 0 and variance $\sigma^2 I$. The time constant τ and time step Δt control the dynamics of the RNN.

Equation 9 defines the activation of the hidden layer at each time step $t > 0$. The activation u_t is obtained by applying the tanh activation function to the hidden state x_t, introducing non-linearity into the model.

Equation 10 specifies the output of the RNN at each time step t. The output y_t is computed by multiplying the output weights W_{out} with the activation vector u_t. The output y_t represents the estimated position of the agent in x and y coordinates.

3.1 Loss and regularization

Authors repeatedly pointed out the importance of regularization for the emergence of grid-like representations in the hidden layer of the RNN. Hence, the loss function used for training the model consisted of three componenets. Task loss - mean squared error between predicted and target positions. L2 regularization on input and output weights to prevent overfitting. And firing rate regularization to encourage sparsity in the hidden layer activations. The total loss function is defined as follows:

$$\mathcal{L}_{\text{total}} = \mathcal{L}_{\text{task}} + \lambda_{\text{L2}}\, \mathcal{L}_{\text{L2}} + \lambda_{\text{FR}}\, \mathcal{L}_{\text{FR}}$$

$$\mathcal{L}_{\text{task}} = \frac{1}{MTN_{\text{out}}} \sum_{m=1}^{M} \sum_{t=1}^{T} \sum_{k=1}^{N_{\text{out}}} \left(Y_{\text{pred}}^{(m,t,k)} - Y_{\text{target}}^{(m,t,k)}\right)^2$$

$$\mathcal{L}_{\text{L2}} = \frac{1}{NN_{\text{in}}} \sum_{i=1}^{N} \sum_{j=1}^{N_{\text{in}}} (W_{\text{in},ij})^2 + \frac{1}{N_{\text{out}} N} \sum_{k=1}^{N_{\text{out}}} \sum_{i=1}^{N} (W_{\text{out},ki})^2$$

$$\mathcal{L}_{\text{FR}} = \frac{1}{MTN} \sum_{m=1}^{M} \sum_{t=1}^{T} \sum_{i=1}^{N} U_{mti}^2$$

4 Results

The RNN models were trained separately on the triangle and square environment datasets. The training process involved optimizing the total loss function defined in Equation 3.1 using backpropagation through time (BPTT). The models were trained for a total of 1500 epochs, with the training loss being monitored throughout the process. The training loss curves for both models are shown in Figure 3.

Figure 4 shows examples of trajectory predictions made by the RNN models trained on square and triangle environments. Both runs were part of the training data. In both cases, some trajectories were predicted quite well, while others tend to diverge significantly from the ground truth.

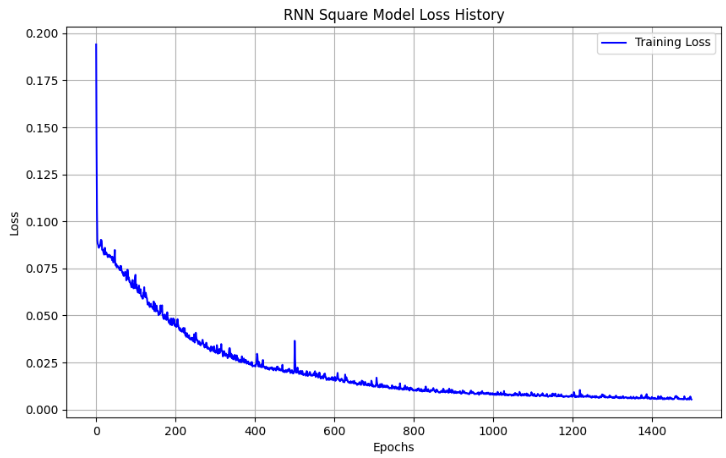

Figure 3: Training loss curves for RNN models trained on a square environment.

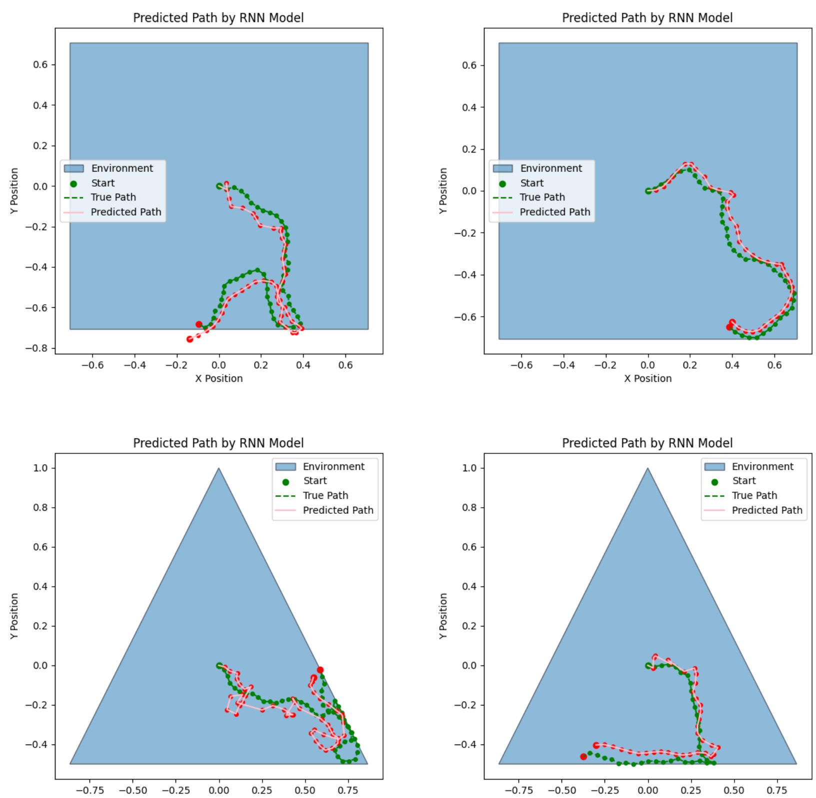

Figure 4: examples of trajectory predictions by RNN models trained on square (top two) and triangle (bottom two) environments.

However, the overall performance of the models shows that they were able to pick up the general trend of the trajectories, but struggled with accurately predicting the exact positions, especially for longer trajectories and trajectories with sharp turns. This indicates that while the models were able to learn some aspects of the path integration task, they were not able to fully capture the complexity of the task.

5 Neuron visualization

To visualize the hidden layer neurons of the trained RNN models, the activations of neurons were recorded for all training data. Further, the activations were turned into heatmaps representing the firing rate of each neuron at different spatial locations. The heatmaps were normalized and smoothed using a Gaussian filter to reduce noise and enhance the visibility of patterns.

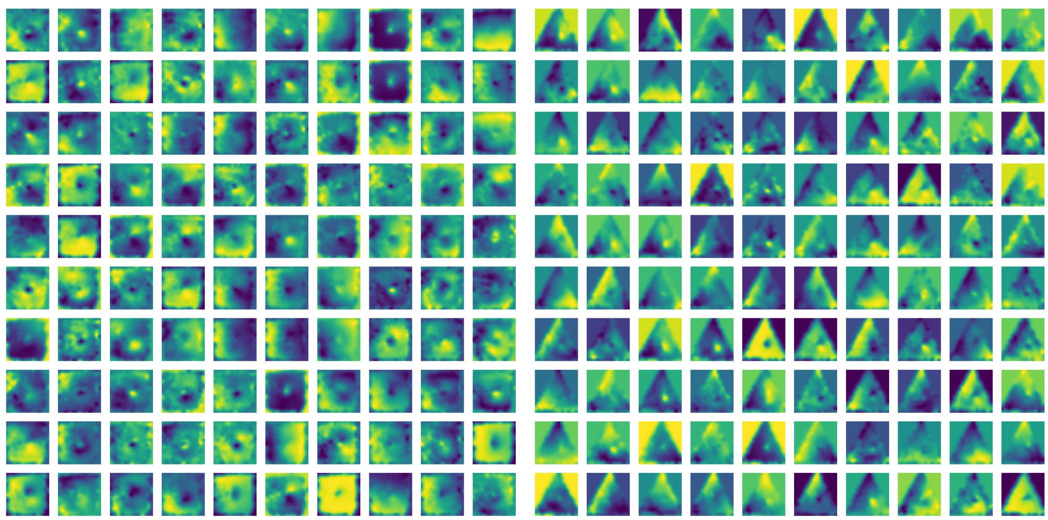

Figure 5: Spatial firing rate maps of hidden layer neurons in the RNN model trained on square (left) and triangle (right) environments.

The visualizations of the hidden layer neurons for the RNN model trained on the square environment are shown in Figure 5. Each subplot represents the spatial firing rate map of a single neuron in the hidden layer. The color intensity indicates the firing rate, with warmer colors representing higher firing rates. As the values were normalized, one can see that for triangle environment out of bounds firings values are different. In reality, there is no data outside of the environment, however, zero could be a high or a low value after normalization, depending on the general trend.

Unfortunately, most of the neurons exhibit diffuse and non-specific firing patterns. However, there still are clear examples of border cells, which fire preferentially along the boundaries of the environment.

A lot of neurons have a distinctive rate of fire for the middle of the environment, this is likely due to the initialization of the agent at the center of the environment for all trajectories. This behavior can be seen as an overfitting to the training data.

Furthermore, no neurons exhibit clear grid cell behavior. Some of them have multiple distinct firing points along the environment, however, the points do not seem to aligned in any strict pattern.

6 Discussion

Clearly the replication of the original paper by (Chaplot et al., 2018), has not been entirely successful. While the RNN was able to pick up the general grasp of the task, the neuron firing rates did not exhibit a similar grid cell behavior.

There are multiple factors contributing to the results of this project. First of all, the data generation procedure could have been replicated closely, due to the lack of information. Even though, the presented approach seems plausible, it might have some subtle but major differences to the original data.

Second of all, due to the time constraints, the models have not been fine tuned well enough. The sequential data causes the training procedure to be inefficient. Training such model for 1500 epochs on 1000 trajectories takes approximately 10 hours. Therefore, only a limited number of hyperparameter combinations could have been tried out.

Finally, a number of small deviations from the original approach could have build up. Causing the results to greatly differ from the initial paper.

6.1 Future work

To further improve the results of this project, several steps can be taken. First of all, the data generation procedure can be refined to more closely match the original paper. This could involve experimenting with different motion models or trajectory generation techniques.

Second of all, no cross validation has been performed to tune the hyperparameters of the model. A more systematic approach to hyperparameter tuning could lead to better model performance. However, better accuracy on the data does not guarantee that the neuron firing patterns will exhibit grid cell behavior.

Finally, more complex environments can be explored, as well as different RNN architectures. This could involve experimenting with deeper networks, different activation functions, or alternative training procedures.

References

Chaplot, D. S., Parisotto, E., & Salakhutdinov, R. (2018). Active neural localization. *arXiv preprint arXiv:1801.08214*.

Hafting, T., Fyhn, M., Molden, S., Moser, M.-B., & Moser, E. I. (2005). Microstructure of a spatial map in the entorhinal cortex. *Nature*, *436*(7052), 801–806.

Mykhalievskyi, T. (2025). *Source code for seminar project.* Retrieved from `https://github.com/GAtemROU/rnn-path-integration`